

# Rethinking Entropy Interventions in RLVR: An Entropy Change Perspective

Zhezheng Hao<sup>1\*</sup> Hong Wang<sup>2\*</sup> Haoyang Liu<sup>3</sup> Jian Luo<sup>3</sup>

Jiarui Yu<sup>2</sup> Hande Dong<sup>2†</sup> Qiang Lin<sup>2</sup> Can Wang<sup>1</sup> Jiawei Chen<sup>1†</sup>

<sup>1</sup> Zhejiang University <sup>2</sup> Tencent <sup>3</sup> University of Science and Technology of China

## Abstract

While Reinforcement Learning with Verifiable Rewards (RLVR) can enhance LLM reasoning, its training process carries a critical risk: entropy collapse. This phenomenon is a rapid decrease in policy entropy, which severely limits exploration and diminishes learning effectiveness. Recent methods attempt to mitigate this collapse by several heuristic entropy interventions, yet their underlying mechanisms on entropy remain unclear. In this work, we conduct a theoretical and quantitative analysis of GRPO’s entropy dynamics, revealing that token-level entropy change in each update step is jointly governed by four key factors: clipping strategy, advantage, token probability, and token entropy. These findings not only explain the mechanisms of existing methods, but also reveal their limitations: they rely on heuristic adjustments to one or two factors on entropy change, leaving other relevant factors unconsidered, which reduces their effectiveness. This motivates us to propose a new method, STEER, which adaptively reweights tokens based on their estimated entropy change to regulate entropy in a principled manner. Experiments on both math and coding benchmarks demonstrate that STEER effectively mitigates entropy collapse and consistently outperforms state-of-the-art baselines.<sup>1</sup>

## 1 Introduction

Reinforcement Learning with Verifiable Rewards (RLVR) has emerged as a powerful paradigm to improve the reasoning abilities of Large Language Models (LLMs) (Zhang et al., 2025a; Jaech et al., 2024; Lambert et al., 2024; Shao et al., 2024). Among existing RLVR algorithms, Group Relative Policy Optimization (GRPO)(Shao et al., 2024) has

become one of the most representative and widely adopted approaches. GRPO optimizes LLM policies using comparable advantage scores computed within groups of sampled instances, and has been instrumental in training strong practical reasoning models (Yang et al., 2025a; Liu et al., 2025a).

Despite its empirical success, GRPO suffers from a major obstacle known as entropy collapse, a sharp decrease of policy entropy during training (Wu et al., 2025; Song et al., 2025; Li et al., 2025; Cui et al., 2025b). Such rapid entropy decrease not only severely impairs exploration, limiting the model’s ability to discover diverse and potentially higher-quality solutions; but also reduces the distinctiveness of the computed advantages, thereby undermining GRPO’s training effectiveness. This raises an important research question: *how can policy entropy be effectively modulated to preserve exploration?*

Several attempts have been made to address entropy collapse, which can be broadly classified into three categories: 1) *Clip-Higher*, which increases the upper bound of the importance-sampling ratio (Yu et al., 2025); 2) *Positive-Reweighting*, which reduces the weight of positive samples with high predictive probability (Zhu et al., 2025; He et al., 2025a); 3) *Entropy-Aware Advantage*, which assigns larger advantage to tokens with large entropy (Cheng et al., 2025; Tan and Pan, 2025; Wang et al., 2025c,b; Deng et al., 2025). While these strategies can alleviate entropy collapse to some extent in practice, they are largely heuristic, lack principled guidance, and the mechanisms behind their entropy effects remain poorly understood. Consequently, their effectiveness is limited, and entropy remains only loosely controlled.

To gain a comprehensive understanding of GRPO’s entropy dynamics and the mechanisms of recent entropy-intervention strategies, we conduct both theoretical and empirical analyses on entropy change under a single training step. Our analy-

\*Equal Contribution.

†Corresponding Authors (donghd66@gmail.com, sleepy-hunt@zju.edu.cn)

<sup>1</sup>Code is available at <https://github.com/zz-haooo/STEER>.

ses operate at a fine-grained, token-level resolution rather than relying solely on coarse-grained global expectation results. While one prior study (Cui et al., 2025b) has investigated GRPO’s entropy behavior, it relies on unrealistic assumptions that result in inaccurate entropy estimates (see Section 3.1). Moreover, it does not explain the mechanisms underlying existing entropy–intervention methods. In contrast, our analyses lead to two main insights: 1) we derive an approximate expression for token-level entropy change, showing that it is determined by four key factors — clipping strategy, advantage, token probability, and conditional entropy. We further clarify how existing methods influence these factors, thereby explaining their empirical success. 2) We identify limitations in prior approaches: their modulation is applied only to a small subset of tokens, neglecting others that may also experience severe entropy collapse; and they consider only partial factors, which reduces their effectiveness and can even accelerate entropy decay in some cases.

Motivated by these findings, we introduce **STEER** (Stabilizing Token-level Entropy-changE via Reweighting), a principled entropy-modulation strategy derived directly from our theoretical analysis. STEER adaptively down-weights tokens with excessively large entropy change, thereby regulating per-step entropy changes and steering the policy toward sustained exploration. Extensive experiments across multiple LLM reasoning benchmarks demonstrate that STEER achieves substantial performance gains while maintaining well-controlled entropy dynamics.

In summary, our contributions are:

- We present a comprehensive analysis of token-level entropy dynamics in GRPO and uncover the mechanisms behind recent entropy-intervention strategies.
- We propose a theoretical-driven strategy that adaptively reweights tokens to regulate per-step token-level entropy changes.
- We conduct extensive experiments on six math and three code benchmarks to demonstrate the effectiveness of the proposed method.

## 2 Preliminaries

### 2.1 RLVR Algorithms

Given a query  $q$  sampled from a dataset  $\mathcal{D}$ , let  $\pi_\theta$  be the policy model and  $o$  be a response sampled from

the policy model. PPO (Schulman et al., 2017) optimizes the policy by maximizing the expected advantage and stabilizes the training process through the clipped surrogate. GRPO (Shao et al., 2024) removes the value model and instead samples a group of rollouts  $\{o_i\}_{i=1}^G$  for query  $q$ , estimating advantages from relative rewards within the group:

$$A_{i,t} = \frac{R_i - \text{mean}(\{R_i\}_{i=1}^G)}{\text{std}(\{R_i\}_{i=1}^G)},$$

where  $R_i \in \{1, -1\}$  indicates whether the  $i$ -th response is correct and the advantage  $A_{i,t}$  is shared across all tokens in that response. Following the token-level formulation in (Yu et al., 2025), GRPO maximizes the following objective:

$$\mathcal{J}(\theta) = \mathbb{E}_{\substack{q \sim \mathcal{D}, \\ \{o_i\}_{i=1}^G \sim \pi_{\text{old}}(\cdot|q)}} \left[ \frac{1}{L} \sum_{i=1}^G \sum_{t=1}^{|o_i|} \min \left( r_{i,t} A_{i,t}, \text{clip}(r_{i,t}, 1 - \varepsilon, 1 + \varepsilon) A_{i,t} \right) \right]. \quad (1)$$

where  $r_{i,t} = \frac{\pi_\theta(o_{i,t}|q, o_{i,<t})}{\pi_{\text{old}}(o_{i,t}|q, o_{i,<t})}$  denotes the importance sampling ratio and  $L = \sum_{i=1}^G |o_i|$  denotes the sum of response lengths within a group. Here we follow (Shao et al., 2024) and omit the KL divergence term from the original GRPO formulation. This modification has been shown to yield better performance and encourage broader exploration.

### 2.2 Policy Entropy of LLMs

Shannon entropy quantifies the uncertainty of a policy model’s action selection given a state (Haarnoja et al., 2018). For LLMs, entropy can be quantified at each generation step. For each sampled response  $o_i$  and step  $t$ , the next-token entropy under policy  $\pi_\theta$  is:

$$\mathcal{H}(q, o_{i,<t}) = -\mathbb{E}_{a \sim \pi_\theta(\cdot|q, o_{i,<t})} [\log \pi_\theta(a | q, o_{i,<t})].$$

The global policy entropy evaluates the model’s generation uncertainty over a query dataset, which can be estimated by averaging token-level entropies over sampled responses:

$$\mathcal{H}(\mathcal{D}) = \mathbb{E}_{\substack{q \sim \mathcal{D}, \\ \{o_i\} \sim \pi_{\text{old}}(\cdot|q)}} \frac{1}{L} \sum_{i=1}^G \sum_{t=1}^{|o_i|} \mathcal{H}_{i,t}.$$

Although  $\mathcal{H}(\pi_\theta, \mathcal{D})$  is data-dependent, it can reflect the diversity of model’s responses across data (detailed in Appendix C.1). Therefore, we use  $\mathcal{D} = \mathcal{D}_{\text{train}}$  when computing policy entropy.

### 3 Entropy-intervention Mechanism: An Entropy Change Perspective

In this section, we present a comprehensive analysis of entropy change within a single training step. Our investigation is conducted at a fine-grained token level, which enables precise monitoring of entropy dynamics and clarifies the mechanisms underlying existing entropy-intervention methods.

#### 3.1 Quantitative Analysis on Entropy Change

To quantitatively characterize the per-token entropy change after one update, we rewrite the GRPO policy gradient (Eq. (1)) as

$$\nabla_{\theta} J(\theta) = \mathbb{E}_{\substack{q \sim \mathcal{D}, \\ \{o_i\}_{i=1}^G \sim \pi_{\text{old}}(\cdot|q)}} \left[ \frac{1}{L} \sum_{i=1}^G \sum_{t=1}^{|o_i|} \mathbb{I}_{\text{clip}} r_{i,t} A_{i,t} \nabla_{\theta} \log \pi_{\theta}(o_{i,t} | q, o_{i,<t}) \right].$$

where the clipping indicator  $\mathbb{I}_{\text{clip}}$  is derived from the ratio clipping operation and is defined as:

$$\mathbb{I}_{\text{clip}} = \begin{cases} 0, & A_{i,t} > 0 \text{ and } r_{i,t} > 1 + \varepsilon, \\ 0, & A_{i,t} < 0 \text{ and } r_{i,t} < 1 - \varepsilon, \\ 1, & \text{otherwise.} \end{cases}$$

For notational convenience, we abbreviate  $\pi_{\theta}(a | s)$  as  $\pi_{\theta}$  and  $A(s, a)$  as  $A$ , and denote the context (state) by  $s \triangleq (q, o_{i,<t})$ . Then we derive the following theorem on token-level entropy change.

**Theorem 1.** *For a logit-independent policy model  $\pi_{\theta}$ , trained using GRPO with a learning rate  $\eta$ , the change of the token-level entropy on state  $s$  between two consecutive steps can be approximated as:*

$$\Omega(s) \triangleq -\frac{\eta}{L} \mathbb{E}_{\pi_{\theta}(\cdot|s)} \left[ \frac{\mathbb{I}_{\text{clip}} A}{\pi_{\text{old}}} \pi_{\theta}(1 - \pi_{\theta}) (\log \pi_{\theta} + \mathcal{H}(s)) \right]. \quad (2)$$

where the approximation error is bounded by  $O(\eta^2)$ , with  $\eta$  typically small ( $< 1e-4$ ) in practice.

The proof is presented in Appendix F.

**Remark 1:** While there is a prior work (Cui et al., 2025b) that also considers entropy change, it assumes a uniform entropy distribution across different queries within the same batch. However, this assumption is rarely attainable in practice, which incurs inaccurate approximation of the ground-truth

entropy change. To quantify, we compare our entropy change estimation with their estimation (denoted as  $\text{Cov}$ ) during a standard GRPO training process. Table 7 reports the Mean Squared Error ( $MSE$ ), Pearson Correlation Coefficient ( $PCC$ ), and Spearman’s Rank Correlation Coefficient ( $SRCC$ ) between ground-truth entropy change and estimation. Across all three metrics,  $\Omega(s)$  delivers orders-of-magnitude lower  $MSE$  and substantially higher  $PCC$  and  $SRCC$  than  $\text{Cov}$ .

Model	Method	$MSE \downarrow$	$PCC \uparrow$	$SRCC \uparrow$
Math-1.5B	$\text{Cov}$	5.37	-6e-5	+0.04
	<i>Ours</i>	5e-4	+0.42	+0.65
7B	$\text{Cov}$	0.53	+0.05	+0.08
	<i>Ours</i>	8e-4	+0.39	+0.72
Math-7B	$\text{Cov}$	0.29	+0.03	+0.06
	<i>Ours</i>	4e-4	+0.42	+0.61

Table 1: Comparison of MSE, PCC and SRCC between covariance-based estimator ( $\text{Cov}$ ) and ours.

**Remark 2:** Theorem 1 implies token-level entropy change is jointly determined by multiple factors: ① the clip indicator  $\mathbb{I}_{\text{clip}}$ , which prevents the entropy change of the tokens with overly large or small importance sampling ratio; ② the advantage  $A$  and the old-policy term  $\pi_{\text{old}}$ , which act as weighting factors for entropy change; ③ the token generation probability  $\pi_{\theta}$  and ④ the token entropy  $\mathcal{H}(s)$  of current state. The contribution of  $\pi_{\theta}$  and  $\mathcal{H}(s)$  to entropy change can be expressed with the following function:

$$\delta(\pi_{\theta}, \mathcal{H}) \triangleq -\pi_{\theta}(1 - \pi_{\theta}) [\log(\pi_{\theta}) + \mathcal{H}(s)].$$

Figure 1 illustrates the impact of the current policy  $\pi_{\theta}$  and entropy  $\mathcal{H}(s)$  on the function  $\delta(\pi_{\theta}, \mathcal{H}(s))$ .

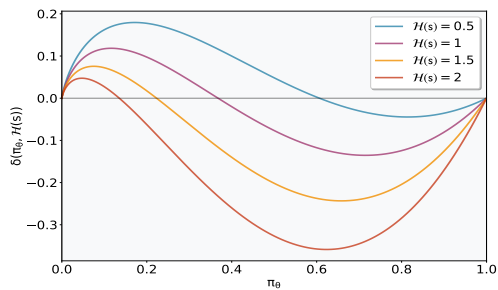


Figure 1:  $\delta$  as a function of  $\pi_{\theta}$  and  $\mathcal{H}(s)$ .

**Remark 3:** We further investigate the direction of entropy change (increase or decrease), which is controlled by the joint effect of the advantage and

token probability. Given that the function  $\delta(\pi_\theta, \mathcal{H})$  takes negative values for high-probability tokens and positive values for low policy probability, we conceptualize this joint effect in terms of four qualitative quadrants in the  $(A, \pi_\theta)$  space shown in Figure 2:

**Quadrant I: Exploitation (entropy decrease).** For high-probability tokens in correct outputs ( $A > 0, \delta < 0$ ), rewarding a well-learned behavior concentrates probability mass, thus *decreasing* entropy.

**Quadrant II: Exploration (entropy increase).** For low-probability tokens in correct outputs ( $A > 0, \delta > 0$ ), rewarding a rare-but-correct behavior diversifies the policy, thereby *increasing* entropy.

**Quadrant III: Suppression (entropy decrease).** For low-probability tokens in incorrect outputs ( $A < 0, \delta > 0$ ), promoting exploration of alternative responses and thereby *increasing* entropy.

**Quadrant IV: Error-Correction (entropy increase).** For high-probability tokens in incorrect outputs ( $A < 0, \delta < 0$ ), penalizing overconfident errors flattens the distribution to encourage seeking alternatives and tends to *increase* entropy.

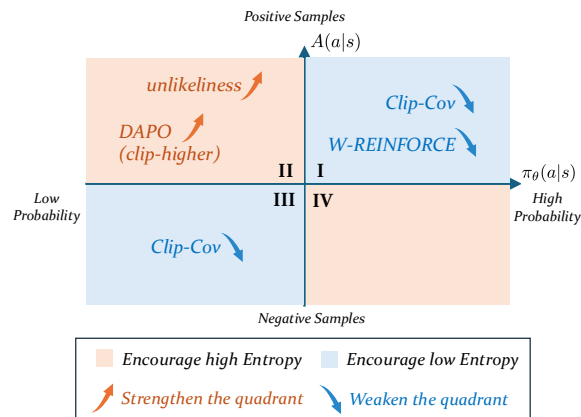


Figure 2: Four-quadrant view of entropy change direction in the advantage–probability plane. The red/blue arrows respectively strengthen/weaken the corresponding quadrant’s entropy effect. Existing methods mapped to the quadrants where they intervene.

We further perform empirical analyses by intervening in the samples on each quadrant. Our empirical observations are closely aligned with our theoretical findings. Readers may refer to Appendix C.3 for additional details.

In a standard RLVR process, these four quadrant-level dynamics co-exist as competing forces that shape the policy. The global policy entropy evolves from the combined effect of these com-

peting updates. Consequently, entropy collapse can be understood as a state where the exploitation-driven, entropy-decreasing updates (Quadrants I and III) consistently overwhelm the exploration-driven, entropy-increasing updates (Quadrants II and IV).

## 4 Analyses on Existing Entropy-Intervention Methods

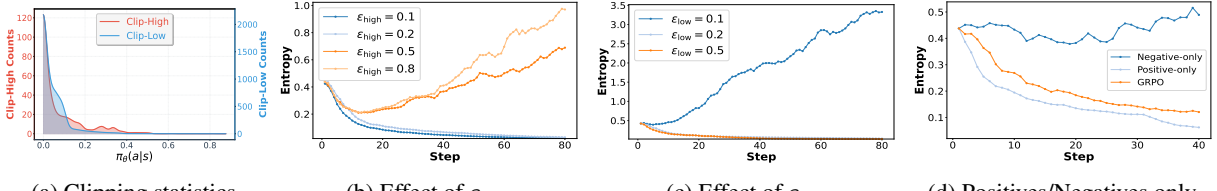
Building on the above theoretical findings, we conduct a comprehensive analysis of existing entropy-intervention techniques, with the aim of revealing their underlying mechanisms and limitations.

**Entropy Effect of Clip-Higher.** Recent work (Yu et al., 2025) considers to decouple the lower and higher clipping bounds with  $\varepsilon_{\text{high}}$  and  $\varepsilon_{\text{low}}$ , and demonstrate that increasing  $\varepsilon_{\text{high}}$  can mitigate entropy collapse.

**Mechanism:** The underlying mechanism can be explained as follows: from the importance ratio  $r = \frac{\pi_\theta}{\pi_{\text{old}}}$ , the ratio is more likely to attain a large value when  $\pi_{\text{old}}$  is relatively small. Consequently, clipping is predominantly triggered for low-probability tokens, a phenomenon confirmed by our empirical observations in Figure 3a, which counts the clipping events in the first 10 steps of GRPO. In this case, the clipping via  $\varepsilon_{\text{high}}$  acts as a filter that removes a considerable number of low-probability positive samples, which typically fall within Quadrant II. Increasing  $\varepsilon_{\text{high}}$  therefore reduces the number of filtered instances, allowing more samples to contribute to entropy increase, thereby mitigating collapse. A similar reasoning applies to the role of  $\varepsilon_{\text{low}}$ : increasing  $\varepsilon_{\text{low}}$  filters fewer instances in Quadrant III which in turn exacerbates entropy collapse.

**Empirical Evidence:** We further validate these observations through empirical experiments. Figure 3b and Figure 3c illustrate the impact of varying  $\varepsilon_{\text{high}}$  and  $\varepsilon_{\text{low}}$ . We observe that increasing  $\varepsilon_{\text{high}}$  can mitigate even reverse entropy collapse, while increasing  $\varepsilon_{\text{low}}$  intensifies collapse.

**Limitation:** Briefly, the effect of tuning clipping thresholds on entropy dynamics can be interpreted as reweighting tokens in Quadrant II and Quadrant III in Figure 2. However, such heuristic methods remain coarse-grained: DAPO, for example, seeks to affect entropy by controlling the updates of some tokens in Quadrant II, without explicitly controlling tokens in other quadrants.



(a) Clipping statistics.

(b) Effect of  $\varepsilon_{\text{high}}$ (c) Effect of  $\varepsilon_{\text{low}}$ 

(d) Positives/Negatives only

Figure 3: Empirical validation of entropy-change mechanisms via ratio clipping and PSR/NSR reweighting.

**Entropy Effect of Re-weighting Positives.** Recent studies have shown that re-weighting positive samples can mitigate entropy collapse. For example, unlikeness (He et al., 2025a) up-weighting tokens in Quadrant II and down-weighting tokens in Quadrant I, while W-REINFORCE (Zhu et al., 2025) down-weighting all positives in training.

**Mechanism:** The effect of unlikeness is clear from Figure 2: it strengthens the entropy-increasing quadrant and weakens entropy-decreasing quadrant, thereby increasing policy entropy. As for W-REINFORCE, the key insight is that token-level updates are dominated by high-probability tokens since they are more likely to be sampled in reasoning. Therefore, down-weighting all positives primarily weakens the entropy-decreasing contribution from Quadrant I, thereby increasing policy entropy.

**Empirical Evidence** To validate this mechanism, we conduct positive-only and negative-only experiments in GRPO setting, where the policy is trained using only positive or only negative samples, respectively. The results, shown in Figures 3d are consistent with the mechanism: training only on positive samples rapidly collapses policy entropy, while training only on negative samples sustains consistently high entropy.

**Limitation:** While these positive re-weighting methods improve global entropy, they only reweight a subset of tokens, leaving the remaining tokens still vulnerable to entropy collapse.

**Entropy Effect of Entropy-aware Advantage.** Several studies have proposed incorporating entropy-related terms into the advantage function to mitigate entropy collapse, such as Entro. Adv. (Cheng et al., 2025) and GTPO (Tan and Pan, 2025). Such methods typically assign larger advantages to tokens with higher entropy. However, our findings indicate that these methods are not universally effective; in fact, they can sometimes accelerate entropy collapse rather than prevent it.

**Mechanism:** As shown by  $\delta(a|s)$  as a function of

$\mathcal{H}(\pi_\theta | s)$  in Figure 4a, high-entropy tokens tend to induce larger changes in entropy. Consequently, assigning greater advantages to high-entropy tokens amplifies their influence. If these tokens tend to decrease entropy, their amplified contribution intensifies the collapse instead of mitigating it.

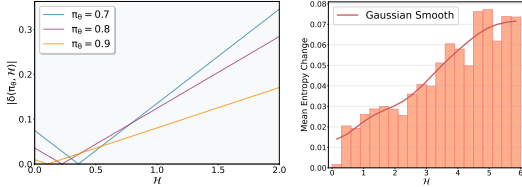
**Empirical Evidence:** We validate this mechanism by examining the entropy dynamics of these methods in Figure 5: compared to the standard GRPO baseline, Entro. Adv. and GTPO both exhibit faster entropy collapse when the policy enters an entropy-decreasing phase. When policy entropy starts to decline, these methods can even accelerate entropy collapse.

**Limitation:** This finding highlights a key flaw in these methods: rather than reliably encouraging exploration, they may instead aggravate entropy decline.

**Limitations of Existing Methods.** While the aforementioned entropy-intervention strategies can partly alleviate entropy collapse in practice, they remain largely heuristic and lack principled guidance. These strategies involve only qualitative adjustments to one or two factors in Eq. 2, leaving other relevant factors unconsidered and failing to capture their joint impacts on the entropy dynamics. As a result, there is a substantial gap between their interventions and the actual entropy evolution observed during training. Their effective is compromised.

## 5 Stabilizing Token-level Entropy-change via Reweighting

The preceding analysis motivates us to develop a more fine-grained and theoretically-driven strategy, termed STEER. The key idea is to introduce an adaptive weight  $\lambda(s)$  for each token in GRPO to regulate its entropy change. With STEER, the entropy change associated with each token is modulated from  $\Omega(s)$  to  $\lambda(s)\Omega(s)$ , thus enabling fine-grained, per-token entropy modulation rather than only monitoring the global expectation as in



(a) Theoretical correlation. (b) Empirical behavior.

Figure 4: Entropy and entropy change.

Method	$\mathbb{I}_{\text{clip}}$	$\pi_\theta$	$A$	$\mathcal{H}(s)$
DAPO	✓	✗	✗	✗
Unlikeliness	✗	✓	✓	✗
W-REINFORCE	✗	✗	✓	✗
Entropy Adv.	✗	✗	✓	✓
KL Reg.	✗	✓	✗	✗
Entropy Reg.	✗	✗	✗	✓
Edge-GRPO	✗	✗	✗	✓
Forking Tokens	✗	✗	✗	✓
Clip-Cov	✗	✓	✓	✗
<b>STEER</b>	✓	✓	✓	✓

Table 2: Factors are considered by existing works and ours.

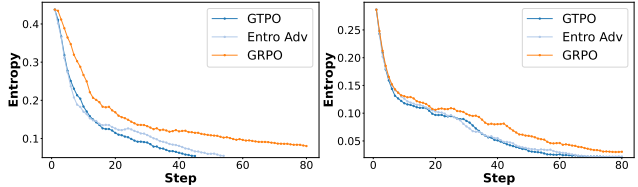
prior methods.

The central question becomes how to design a suitable  $\lambda(s)$ . Naturally,  $\lambda(s)$  should vary according to  $\Omega(s)$  — larger entropy changes indicate a higher risk of entropy collapse and should be attenuated. To achieve this, we employ an exponential decay function:

$$\lambda(s) = \exp\left(\alpha \frac{|\Omega(s)|}{\max_{s \in \mathcal{B}} |\Omega(s)|}\right), \quad (3)$$

where  $\alpha < 0$  is the hyperparameter controlling the decay rate. This formulation satisfies two desired properties: (1) it is monotonically decreasing with respect to the normalized entropy change; (2) the introduction of the exponential ensures that all weights remain strictly positive. We apply the absolute value  $|\Omega(s)|$  to measure the magnitude of entropy-change, since large entropy increases may also be sub-optimal. Controlling both increases and decreases within a stable range leads to more stable training dynamics. The normalization by the batch maximum ensures numerical stability across varying magnitudes of entropy change.

A hyperparameter  $\alpha$  governs the slope of the decay curve. Equivalently,  $\alpha$  determines the minimum attainable weight,  $\lambda_{\min} = \exp(-\alpha)$ . Thus,



(a) Math-7B on DAPO-17k (b) Math-7B on Math

Figure 5: Entropy dynamics with advantage shaping.

Eq.( 3) can be understood as an inverse mapping of entropy changes into the range  $[\lambda_{\min}, 1]$ , with larger entropy changes corresponding to smaller weights. In practice, we find it more convenient to tune  $\lambda_{\min}$  directly, rather than  $\alpha$ , due to its better interpretability in controlling the minimum modulation weight.

## 6 Experiments

**Training and Evaluation** We conduct experiments on three different models, including Qwen2.5-Math-7B, Qwen2.5-Math-1.5B and Qwen2.5-14B. We adapt our training codebase from verl (Sheng et al., 2025) and follow the training recipe of standard GRPO. Our training data is DAPO-Math-17k (Yu et al., 2025), containing only math problems with integer ground-truth answers. We evaluate our models and baselines on six widely used mathematical reasoning benchmarks: AIME24, AIME25, AMC23, MATH-500, Minerva Math, and OlympiadBench. To ensure the reliability, all results reported in the main experiments are averaged over two independent runs. For fair comparison, we adopt the experimental setup used in existing work. Training and evaluation details of our method and baselines are in Appendix D.

**Baselines** For a thorough comparison, we compare our method against 10 baselines, including standard GRPO (Shao et al., 2024), SimpleRL-Zoo (Zeng et al., 2025), Eurus-PRIME (Cui et al., 2025a), OPO (Hao et al., 2025), GRPO with clip-high (Yu et al., 2025), GRPO with entropy loss (Schulman et al., 2017), GRPO with Fork Tokens (Wang et al., 2025c), W-REINFORCE (Zhu et al., 2025), Entro. Adv. (Cheng et al., 2025), Clip-Cov and KL-Cov (Cui et al., 2025b). For all baselines, the default training hyperparameters in RLVR are consistent with STEER, while the newly introduced hyperparameters follow the original implementations, respectively.

Table 3: Benchmark results of different methods. We report avg@32 for AIME24, AIME25, and AMC23 and avg@1 for others. All results are presented as percentages.

Method	AIME24	AIME25	AMC23	MATH500	Minerva	Olympiad	Avg.
Qwen2.5-Math-7B	13.8	5.3	44.6	39.6	9.9	13.8	21.2
<b>Classical RLVR Methods</b>							
GRPO	28.0	14.3	66.2	78.6	37.3	40.9	44.2
SimpleRL-Zoo	30.8	14.2	65.4	79.2	37.1	40.8	44.6
Eurus-PRIME	20.9	13.0	65.2	79.8	37.4	40.6	42.8
OPO	32.2	13.4	71.5	82.2	38.2	41.0	46.4
<b>Entropy Intervention Methods</b>							
GRPO w/ clip-high	31.7	12.8	66.8	79.0	38.6	39.3	44.7
GRPO w/ Entro. Loss	29.1	14.0	67.6	80.0	38.2	37.9	44.5
GRPO w/ Fork Tokens	31.9	14.3	65.5	79.2	37.1	40.9	44.8
W-REINFORCE	31.9	14.3	65.5	79.2	37.1	40.9	44.8
Entro. Adv.	27.5	13.5	70.2	79.6	36.8	42.8	45.1
Clip-Cov	32.5	12.9	68.4	78.0	40.8	41.3	45.7
KL-Cov	32.8	14.1	64.2	78.8	37.1	39.4	44.4
<b>STEER (Ours)</b>	<b>36.2</b>	<b>16.1</b>	<b>72.1</b>	<b>82.2</b>	<b>41.7</b>	<b>43.0</b>	<b>48.6</b>

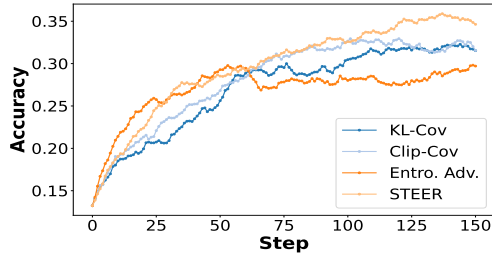


Figure 6: Test accuracy dynamics comparison.

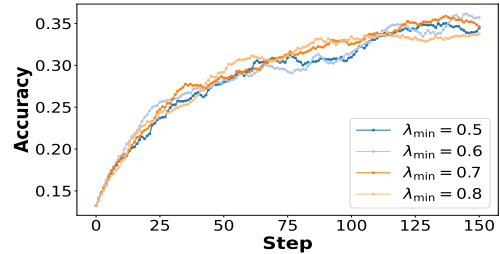


Figure 7: Test accuracy dynamics under different  $\lambda_{\min}$ .

**Main Results** As shown in Table 3, STEER outperforms classical RLVR baselines as well as existing entropy intervention baselines across all datasets. STEER improves average performance by 2.7 points over the second runner-up (OPO) and by 3.4 points over the third runner-up (Clip-Cov) across all baselines. The performance experiments on Qwen2.5-Math-1.5B and Qwen2.5-14B shown in Table 11 are compared with the top three competitors in Table 3 (i.e., OPO, Clip-Cov, and Entro. Adv.). STEER also consistently achieves the highest average performance on both Qwen2.5-Math-1.5B (38.1) and Qwen2.5-14B (45.1), demonstrating its superior capabilities in improving model reasoning.

Figure 6 shows the test curves during training, where STEER outperforms the baselines. Figure 7 presents the test curves for different hyperparameters, demonstrating both stability and superiority.

**Entropy Control** The strength of our method is not only reflected in its performance but also in its ability to regulate entropy across a wide range. We consider an extreme training setup with  $\varepsilon_{\text{high}} = 5$  and  $\varepsilon_{\text{low}} = 0.99$ , where almost no ratio clipping is applied. In such scenarios, RL training is vulnerable due to unstable gradient updates under extreme clipping ratios. The results are shown in the Figure 8. Most methods fail to maintain stable entropy: GRPO and Entro. Adv. tend toward entropy collapse; adding an Entropy Loss drives entropy up rapidly, leading to excessive uncertainty; and Clip-Cov cannot reliably control entropy. By contrast, STEER stabilizes after an initial decline and maintains steady entropy subsequently. The test set results for extreme scenarios are provided in the Appendix E.1. Besides, Figure 9 depicts the trend of average token weight as a function of the absolute token entropy change in the first 10 steps. When

Table 4: Performance on test datasets in extreme scenarios.

Method	AIME24	AIME25	AMC23	MATH500	Minerva	Olympiad	Avg.
GRPO	31.6	12.8	66.7	79.0	39.3	40.1	44.9
Entro. Adv.	34.8	13.4	64.3	77.6	37.6	39.9	44.6
Entro. Loss	32.7	14.7	71.3	79.0	36.8	41.4	46.0
Clip-Cov	30.4	14.0	72.3	79.6	37.1	41.7	45.8
<b>STEER</b>	<b>36.1</b>	<b>16.0</b>	<b>76.3</b>	<b>80.5</b>	<b>39.5</b>	<b>42.3</b>	<b>48.5</b>

entropy changes are small, most weights remain near 1; only tokens with large entropy changes receive substantially reduced weights, indicating that STEER stabilizes training without impeding learning.

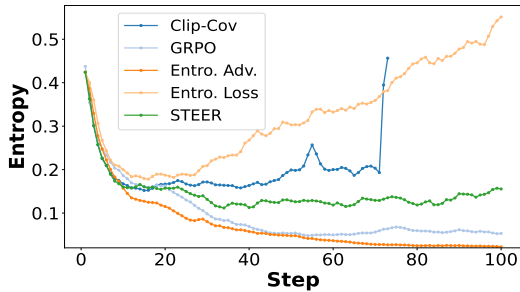


Figure 8: Entropy dynamics in extreme scenarios.

We test entropy intervention methods in uncontrolled training scenarios ( $\varepsilon_{\text{high}} = 5$  and  $\varepsilon_{\text{low}} = 0.99$ ), with test set accuracy shown in Table 10. It can be observed that, even in training scenarios where the clipping operation is almost completely removed, STEER maintains relatively stable performance compared to other entropy intervention methods and achieves the highest accuracy across all test sets.

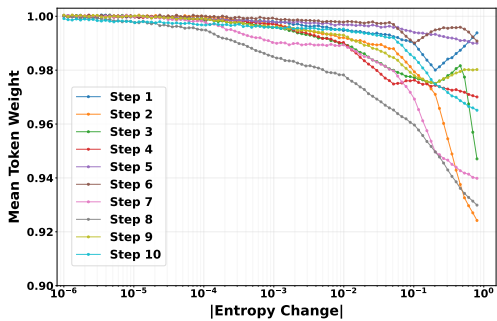


Figure 9: Relationship between mean token weight and entropy change across steps.

**Real-World Code Tasks** Beyond math reasoning, we also evaluate our method on real-world

code tasks, including Code Edit and Code Generation. Detailed training setups are provided in D.2. Figure 5 compares STEER with GRPO on Qwen2.5-coder models: for the Code Edit task we report exact-match accuracy, and for the Code Generation task we report avg@4. Each result is the average of three runs. It can be discovered that STEER exceeds GRPO at least 1% in each model and test set. These results demonstrate the superior performance of STEER in various scenarios.

Test	Method	3B	7B	14B
Internal	GRPO	39.7	40.1	42.6
	STEER	41.2	41.9	45.1
Zeta	GRPO	17.4	22.0	22.3
	STEER	19.3	24.00	24.1
LCB-v5	GRPO	24.4	28.5	29.3
	STEER	24.9	29.2	31.8

Table 5: Performance on real-world coding tasks.

## 7 Conclusion

In this paper, we rethink the entropy interventions through the lens of entropy change. By proposing a quantitative analysis framework for entropy change, the entropy effect of current intervention methods can be unified and elucidated through token-level analysis. Motivated by moderating entropy change, we propose STEER, an adaptive, fine-grained reweighting scheme that precisely keeps per-step entropy changes within a moderate band by suppressing potentially disruptive updates. Extensive experiments on mathematical reasoning and code benchmarks demonstrate that STEER achieves superior performance with enhanced training stability. Our work provides both a new lens for analyzing RL dynamics and a practical solution for developing robust and effective LLM training algorithms.

## 8 Limitation

The empirical study in this work focuses on scenarios where policy entropy decreases during training. In real training pipelines, some models do not exhibit significant entropy collapse (due to their pretraining procedures or subsequent finetuning configurations); such “entropy-stable” models are not covered by this work. In addition, the reinforcement learning experiments in this work are based on verifiable rewards while domains without task-specific verifiers are not discussed.

## References

Daixuan Cheng, Shaohan Huang, Xuekai Zhu, Bo Dai, Wayne Xin Zhao, Zhenliang Zhang, and Furu Wei. 2025. Reasoning with exploration: An entropy perspective. *arXiv preprint arXiv:2506.14758*.

Xiangxiang Chu, Hailang Huang, Xiao Zhang, Fei Wei, and Yong Wang. 2025. Gpg: A simple and strong reinforcement learning baseline for model reasoning. *arXiv preprint arXiv:2504.02546*.

Ganqu Cui, Lifan Yuan, Zefan Wang, Hanbin Wang, Wendi Li, Bingxiang He, Yuchen Fan, Tianyu Yu, Qixin Xu, Weize Chen, and 1 others. 2025a. Process reinforcement through implicit rewards. *arXiv preprint arXiv:2502.01456*.

Ganqu Cui, Yuchen Zhang, Jiacheng Chen, Lifan Yuan, Zhi Wang, Yuxin Zuo, Haozhan Li, Yuchen Fan, Huayu Chen, Weize Chen, and 1 others. 2025b. The entropy mechanism of reinforcement learning for reasoning language models. *arXiv preprint arXiv:2505.22617*.

Jia Deng, Jie Chen, Zhipeng Chen, Wayne Xin Zhao, and Ji-Rong Wen. 2025. Decomposing the entropy-performance exchange: The missing keys to unlocking effective reinforcement learning. *arXiv preprint arXiv:2508.02260*.

Tuomas Haarnoja, Aurick Zhou, Pieter Abbeel, and Sergey Levine. 2018. Soft actor-critic: Off-policy maximum entropy deep reinforcement learning with a stochastic actor. In *International conference on machine learning*, pages 1861–1870. Pmlr.

Yaru Hao, Li Dong, Xun Wu, Shaohan Huang, Zewen Chi, and Furu Wei. 2025. On-policy rl with optimal reward baseline. *arXiv preprint arXiv:2505.23585*.

Andre He, Daniel Fried, and Sean Welleck. 2025a. Rewarding the unlikely: Lifting gpro beyond distribution sharpening. *arXiv preprint arXiv:2506.02355*.

Chaoqun He, Renjie Luo, Yuzhuo Bai, Shengding Hu, Zhen Leng Thai, Junhao Shen, Jinyi Hu, Xu Han, Yujie Huang, Yuxiang Zhang, and 1 others. 2024. Olympiadbench: A challenging benchmark for promoting agi with olympiad-level bilingual multimodal scientific problems. *arXiv preprint arXiv:2402.14008*.

Jujie He, Jiacai Liu, Chris Yuhao Liu, Rui Yan, Chaojie Wang, Peng Cheng, Xiaoyu Zhang, Fuxiang Zhang, Jiacheng Xu, Wei Shen, and 1 others. 2025b. Sky-work open reasoner 1 technical report. *arXiv preprint arXiv:2505.22312*.

Dan Hendrycks, Collin Burns, Saurav Kadavath, Akul Arora, Steven Basart, Eric Tang, Dawn Song, and Jacob Steinhardt. 2021. Measuring mathematical problem solving with the math dataset. *arXiv preprint arXiv:2103.03874*.

Jingcheng Hu, Yinmin Zhang, Qi Han, Daxin Jiang, Xiangyu Zhang, and Heung-Yeung Shum. 2025. Open-reasoner-zero: An open source approach to scaling up reinforcement learning on the base model. *arXiv preprint arXiv:2503.24290*.

Aaron Jaech, Adam Kalai, Adam Lerer, Adam Richardson, Ahmed El-Kishky, Aiden Low, Alec Helyar, Aleksander Madry, Alex Beutel, Alex Carney, and 1 others. 2024. Openai o1 system card. *arXiv preprint arXiv:2412.16720*.

Naman Jain, King Han, Alex Gu, Wen-Ding Li, Fanjia Yan, Tianjun Zhang, Sida Wang, Armando Solar-Lezama, Koushik Sen, and Ion Stoica. 2024. Live-codebench: Holistic and contamination free evaluation of large language models for code. *arXiv preprint arXiv:2403.07974*.

Nathan Lambert, Jacob Morrison, Valentina Pyatkin, Shengyi Huang, Hamish Ivison, Faeze Brahman, Lester James V Miranda, Alisa Liu, Nouha Dziri, Shane Lyu, and 1 others. 2024. Tulu 3: Pushing frontiers in open language model post-training. *arXiv preprint arXiv:2411.15124*.

Aitor Lewkowycz, Anders Andreassen, David Dohan, Ethan Dyer, Henryk Michalewski, Vinay Ramasesh, Ambrose Slone, Cem Anil, Imanol Schlag, Theo Gutman-Solo, and 1 others. 2022. Solving quantitative reasoning problems with language models. *Advances in neural information processing systems*, 35:3843–3857.

Jia Li, Edward Beeching, Lewis Tunstall, Ben Lipkin, Roman Soletskyi, Shengyi Huang, Kashif Rasul, Longhui Yu, Albert Q Jiang, Ziju Shen, and 1 others. 2024. Numinamath: The largest public dataset in ai4maths with 860k pairs of competition math problems and solutions. *Hugging Face repository*, 13(9):9.

Qingbin Li, Rongkun Xue, Jie Wang, Ming Zhou, Zhi Li, Xiaofeng Ji, Yongqi Wang, Miao Liu, Zheming Yang, Minghui Qiu, and 1 others. 2025. Cure: Critical-token-guided re-concatenation for entropy-collapse prevention. *arXiv preprint arXiv:2508.11016*.

Aixin Liu, Aoxue Mei, Bangcai Lin, Bing Xue, Bingxuan Wang, Bingzheng Xu, Bochao Wu, Bowei Zhang, Chaofan Lin, Chen Dong, and 1 others. 2025a. Deepseek-v3. 2: Pushing the frontier of open large language models. *arXiv preprint arXiv:2512.02556*.

Mingjie Liu, Shizhe Diao, Ximing Lu, Jian Hu, Xin Dong, Yejin Choi, Jan Kautz, and Yi Dong. 2025b. Prorl: Prolonged reinforcement learning expands reasoning boundaries in large language models. *arXiv preprint arXiv:2505.24864*.

Michael Luo, Sijun Tan, Justin Wong, Xiaoxiang Shi, William Y Tang, Manan Roongta, Colin Cai, Jeffrey Luo, Tianjun Zhang, Li Erran Li, and 1 others. 2025. Deepscaler: Surpassing o1-preview with a 1.5 b model by scaling rl. *Notion Blog*.

Volodymyr Mnih, Adria Puigdomenech Badia, Mehdi Mirza, Alex Graves, Timothy Lillicrap, Tim Harley, David Silver, and Koray Kavukcuoglu. 2016. Asynchronous methods for deep reinforcement learning. In *International conference on machine learning*, pages 1928–1937. PMLR.

John Schulman, Filip Wolski, Prafulla Dhariwal, Alec Radford, and Oleg Klimov. 2017. Proximal policy optimization algorithms. *arXiv preprint arXiv:1707.06347*.

Zhihong Shao, Peiyi Wang, Qihao Zhu, Runxin Xu, Junxiao Song, Xiao Bi, Haowei Zhang, Mingchuan Zhang, YK Li, Yang Wu, and 1 others. 2024. Deepseekmath: Pushing the limits of mathematical reasoning in open language models. *arXiv preprint arXiv:2402.03300*.

Guangming Sheng, Chi Zhang, Zilingfeng Ye, Xibin Wu, Wang Zhang, Ru Zhang, Yanghua Peng, Haibin Lin, and Chuan Wu. 2025. Hybridflow: A flexible and efficient rlhf framework. In *Proceedings of the Twentieth European Conference on Computer Systems*, pages 1279–1297.

Yuda Song, Julia Kempe, and Remi Munos. 2025. Outcome-based exploration for llm reasoning. *arXiv preprint arXiv:2509.06941*.

Hongze Tan and Jianfei Pan. 2025. Gtpo and grpo-s: Token and sequence-level reward shaping with policy entropy. *arXiv preprint arXiv:2508.04349*.

Haozhe Wang, Qixin Xu, Che Liu, Junhong Wu, Fangzhen Lin, and Wenhui Chen. 2025a. Emergent hierarchical reasoning in llms through reinforcement learning. *arXiv preprint arXiv:2509.03646*.

Jiakang Wang, Runze Liu, Fuzheng Zhang, Xiu Li, and Guorui Zhou. 2025b. Stabilizing knowledge, promoting reasoning: Dual-token constraints for rlvr. *arXiv preprint arXiv:2507.15778*.

Shenzhi Wang, Le Yu, Chang Gao, Chujie Zheng, Shixuan Liu, Rui Lu, Kai Dang, Xionghui Chen, Jianxin Yang, Zhenru Zhang, and 1 others. 2025c. Beyond the 80/20 rule: High-entropy minority tokens drive effective reinforcement learning for llm reasoning. *arXiv preprint arXiv:2506.01939*.

Fang Wu, Weihao Xuan, Ximing Lu, Zaid Harchaoui, and Yejin Choi. 2025. The invisible leash: Why rlvr may not escape its origin. *arXiv preprint arXiv:2507.14843*.

An Yang, Anfeng Li, Baosong Yang, Beichen Zhang, Binyuan Hui, Bo Zheng, Bowen Yu, Chang Gao, Chengan Huang, Chenxu Lv, and 1 others. 2025a. Qwen3 technical report. *arXiv preprint arXiv:2505.09388*.

Shihui Yang, Chengfeng Dou, Peidong Guo, Kai Lu, Qiang Ju, Fei Deng, and Rihui Xin. 2025b. Dcpo: Dynamic clipping policy optimization. *arXiv preprint arXiv:2509.02333*.

Qiying Yu, Zheng Zhang, Ruofei Zhu, Yufeng Yuan, Xiaochen Zuo, Yu Yue, Weinan Dai, Tiantian Fan, Gaohong Liu, Lingjun Liu, and 1 others. 2025. Dapo: An open-source llm reinforcement learning system at scale. *arXiv preprint arXiv:2503.14476*.

Weihao Zeng, Yuzhen Huang, Qian Liu, Wei Liu, Keqing He, Zejun Ma, and Junxian He. 2025. Simplerl-zoo: Investigating and taming zero reinforcement learning for open base models in the wild. *arXiv preprint arXiv:2503.18892*.

Kaiyan Zhang, Yuxin Zuo, Bingxiang He, Youbang Sun, Runze Liu, Che Jiang, Yuchen Fan, Kai Tian, Guoli Jia, Pengfei Li, and 1 others. 2025a. A survey of reinforcement learning for large reasoning models. *arXiv preprint arXiv:2509.08827*.

Ruipeng Zhang, Ya-Chien Chang, and Sicun Gao. 2025b. When maximum entropy misleads policy optimization. *arXiv preprint arXiv:2506.05615*.

Xingjian Zhang, Siwei Wen, Wenjun Wu, and Lei Huang. 2025c. Edge-grpo: Entropy-driven grpo with guided error correction for advantage diversity. *arXiv preprint arXiv:2507.21848*.

Xinyu Zhu, Mengzhou Xia, Zhepei Wei, Wei-Lin Chen, Danqi Chen, and Yu Meng. 2025. The surprising effectiveness of negative reinforcement in llm reasoning. *arXiv preprint arXiv:2506.01347*.

## Contents

<b>A Usage of LLMs</b>	<b>12</b>
<b>B Related work</b>	<b>12</b>
B.1 Entropy-Oriented RL Methods for LLM Reasoning . . . . .	12
B.2 A Token-level Gradient Reweighting Perspective for Shaping Policy Entropy . . . . .	12
<b>C Supplementary Empirical Analysis for RLVR Entropy</b>	<b>13</b>
C.1 Empirical Properties of Policy Entropy . . . . .	13
C.2 Entropy Change Estimation Comparison . . . . .	14
C.3 Influencing Entropy Dynamics by Strengthening or Weakening the Quadrants . . . . .	16
C.4 Entropy Effect of Clipping Operation . . . . .	16
<b>D Training Settings</b>	<b>18</b>
D.1 Detailed Information for dataset . . . . .	18
D.2 Training Details for our method and baselines	18
<b>E Supplementary Performance Evaluation</b>	<b>19</b>
E.1 Performance in Extreme Scenarios . . . . .	19
E.2 Performance Comparison on Different Models	19
E.3 Ablation Study . . . . .	19
<b>F Theorem Proof Details</b>	<b>21</b>

## A Usage of LLMs

Throughout the preparation of this manuscript, Large Language Models (LLMs) were utilized as a writing and editing tool. Specifically, we employed LLMs to improve the clarity and readability of the text, refine sentence structures, and correct grammatical errors. All final content, including the core scientific claims, experimental design, and conclusions, was conceived and written by us, and we take full responsibility for the final version of this paper.

## B Related work

### B.1 Entropy-Oriented RL Methods for LLM Reasoning

Entropy regularization (Mnih et al., 2016; Haarnoja et al., 2018), an early line of work in traditional RL, may mislead actions at critical states (Zhang et al., 2025b) and has been shown to be highly sensitive to the coefficient in LLM training (Cheng et al., 2025; Cui et al., 2025b). (Liu et al., 2025b) argues that the KL penalty preserves entropy and acts as a regularizer, ensuring that the online policy remains close to a stable reference, which stabilizes learning and reduces overfitting to misleading reward signals. Nevertheless, the KL divergence term between the current policy  $\pi_\theta$  and the reference policy  $\pi_{\text{ref}}$  in the original form (Shao et al., 2024) is excluded in our work, since its practical impact is often negligible or counterproductive for reasoning tasks, as demonstrated in recent works (Yu et al., 2025; Chu et al., 2025; Hu et al., 2025). One typical approach to address entropy collapse is by raising the sampling temperature during inference. However, recent findings in (Luo et al., 2025) suggest that while this method postpones the onset of entropy collapse, it does not prevent it, as entropy continues to decrease progressively throughout the training process. Recent studies have sought to mitigate entropy collapse by adjusting key elements of policy optimization, such as PPO-style ratio clipping (Yu et al., 2025; Yang et al., 2025b), balancing positive and negative samples (Zhu et al., 2025), and applying KL regularization (Liu et al., 2025b). However, these methods are broad and lack fine-grained control at the token level, with their mechanisms often not fully explained in a unified or principled way. Several methods attempt to encourage exploration via an entropy-induced advantage (Cheng et al., 2025; Tan and Pan, 2025; Wang et al., 2025c,b; Deng et al., 2025), with the intuition

that emphasizing uncertain states will promote exploration and raise overall policy entropy. In practice, however, we found this design often fails to reliably mitigate entropy collapse because it disproportionately strengthens learning on high-entropy tokens and thereby magnifies entropy change, leading to unreliable entropy control. Although prior work (Cui et al., 2025b) considers entropy change, the resulting estimation is distorted due to its unreasonable state-equivalence assumption. Notably, its entropy-control scheme (i) enforces a hard binary split by entropy change without considering their intra-group differentiation, and (ii) may hinder the learning process, since high-entropy-change tokens that are informative for exploration are over-penalized.

### B.2 A Token-level Gradient Reweighting Perspective for Shaping Policy Entropy

To summarize existing methods more clearly, we reformulate them through the lens of token-level gradients. Existing entropy intervention methods can be unified into a gradient reweighting framework and subsequently examined their respective impacts on policy entropy.

The policy gradient of off-policy optimization can be expressed as follows:

$$\nabla_\theta J(\theta) = \mathbb{E}_{q \sim \mathcal{D}, \{o_i\} \sim \pi_{\text{old}}(\cdot|q)} \left[ \frac{1}{\sum_{i=1}^G |o_i|} \sum_{i=1}^G \sum_{t=1}^{|o_i|} w_{i,t}(q) \nabla_\theta \log \pi_\theta(o_{i,t} | q, o_{i,<t}) \right]. \quad (4)$$

For GRPO in Eq. (1),  $w_{i,t}(q) = \mathbb{I}_{\text{clip}} r_{i,t} A_{i,t}$ , where

$$\mathbb{I}_{\text{clip}} = \begin{cases} 0, & A_{i,t} > 0 \text{ and } r_{i,t} > 1 + \varepsilon, \\ 0, & A_{i,t} < 0 \text{ and } r_{i,t} < 1 - \varepsilon, \\ 1, & \text{otherwise,} \end{cases} \quad (5)$$

where  $r_{i,t} = \frac{\pi_\theta(o_{i,t}|q, o_{i,<t})}{\pi_{\text{old}}(o_{i,t}|q, o_{i,<t})}$  denotes the importance sampling ratio. Advantage  $A_{i,t}$  is calculated by reward  $R_{i,t}$ . For brevity and uniformity, let

$$w_{i,t}(q) = \mathbb{I}_{\text{clip}} r_{i,t} A_{i,t} + \beta \mathcal{R}(\pi_\theta), \quad (6)$$

where  $\mathcal{R}(\pi_\theta)$  is the regularization. Table 6 briefly summarizes existing methods based on their interventions on token-level weight  $w_{i,t}(q)$ . It is evident that existing methods can be categorized into different token-level gradient reweighting schemes,

Method	Intervention
<b>DAPO / DCPO</b> (Yu et al., 2025) (Yang et al., 2025b)	$\mathbb{I}_{\text{clip}} = \begin{cases} 0, & A_{i,t} > 0 \text{ and } r_{i,t} > 1 + \varepsilon_{\text{high}}, \\ 0, & A_{i,t} < 0 \text{ and } r_{i,t} < 1 - \varepsilon_{\text{low}}, \\ 1, & \text{otherwise} \end{cases}$
<b>KL penalty</b> (Shao et al., 2024)	$\mathcal{R}(\pi_\theta) = \frac{\pi_{\text{ref}}(o_{i,t}   q, o_{i,<t})}{\pi_\theta(o_{i,t}   q, o_{i,<t})}$
<b>Entropy Regularization</b> (He et al., 2025b)	$\mathcal{R}(\pi_\theta) = -\log \pi_\theta(o_{i,t}   q, o_{i,<t})$
<b>Unlikeliness</b> (He et al., 2025a)	$\hat{R}_{i,t} = R_{i,t} \left( 1 - \beta_{\text{rank}} \frac{G-\text{rank}(o_i)}{G} \right), \beta_{\text{rank}} > 0$
<b>W-REINFORCE</b> (Zhu et al., 2025)	$\hat{A}_{i,t} = \begin{cases} \lambda, & A_{i,t} > 0 \\ 1, & A_{i,t} < 0 \end{cases}, \lambda < 1$
<b>Entropy Advantage</b> (Cheng et al., 2025)	$\hat{A}_{i,t} = A_{i,t} + \min \left( \alpha \cdot \mathcal{H}_{i,t}^{\text{detach}}, \frac{ A_{i,t} }{\kappa} \right), \alpha > 0, \kappa > 1$
<b>GTPO</b> (Tan and Pan, 2025)	$\hat{R}_{i,t} = R_{i,t} + \alpha \frac{\mathcal{H}_{i,t}}{\frac{1}{d_t} \sum_{k=1}^{d_t} \mathcal{H}_{k,t}}, \text{ for } R_{i,t} > 0$
<b>EDGE-GRPO</b> (Zhang et al., 2025c)	$\hat{A}_i = \frac{A_i}{\hat{\mathcal{H}}_i}, \hat{\mathcal{H}}_i : \text{normalized entropy across the group}$
<b>PPL-based</b> (Deng et al., 2025)	$\hat{A}_{i,t} = A_{i,t} (1 - \alpha \log \text{PPL}(o_i)), \alpha > 0$
<b>Position-based</b> (Deng et al., 2025)	$\hat{A}_{i,t} = A_{i,t} + \gamma \text{sign}(A_{i,t}) \sigma(r_{it}) \quad r_{it} : \text{token's relative position}$
<b>Forking Tokens</b> (Wang et al., 2025c)	$\mathbb{I}_{\text{clip}} = \mathbb{I}_{\text{clip}} \wedge \mathbb{I}(\mathcal{H}_{i,t} > \tau_{\mathcal{B}}), \tau_{\mathcal{B}} : \text{threshold in batch } \mathcal{B}$

Table 6: A Token-level Gradient Reweighting Perspective for Shaping Policy Entropy.

depending on factors such as advantage  $A_{i,t}$ , generation probability  $\pi_\theta(o_{i,t} | q, o_{i,<t})$ , conditional entropy  $\mathcal{H}_{i,t}$ , etc. **These methods can be broadly summarized as increasing or suppressing the training weights of tokens that satisfy certain properties.** Our analysis explains why these methods are effective or not. Our proposed STEER adopts reweighting based on token-level entropy change, which is more fundamental for entropy control. Besides, recent studies (Wang et al., 2025c,a) highlight the importance of high-entropy tokens for reasoning and propose various mechanisms to strengthen their training. This does not conflict with our approach STEER as STEER explicitly controls token entropy changes to avert training collapse while preserving learning on critical tokens. This further confirms why (Zhang et al., 2025c) is effective in mitigating entropy collapse.

## C Supplementary Empirical Analysis for RLVR Entropy

This section presents supplementary experiments that further support the analyses and claims in the main text.

### C.1 Empirical Properties of Policy Entropy

In this subsection, we present several basic empirical properties of policy entropy dynamics in RLVR, providing a global view of how entropy behaves during training.

Figure 10 summarizes several empirical properties of policy entropy in RLVR. First, continuity across batch (panel 1) shows that, under a standard GRPO run, policy entropy decays smoothly step by step and entropy collapse appears as a gradual trend rather than sudden jumps. Second, dependence on model (panel 2) compares different backbones (e.g., Qwen2.5-Math-1.5B / 7B vs. Qwen2.5-7B) and

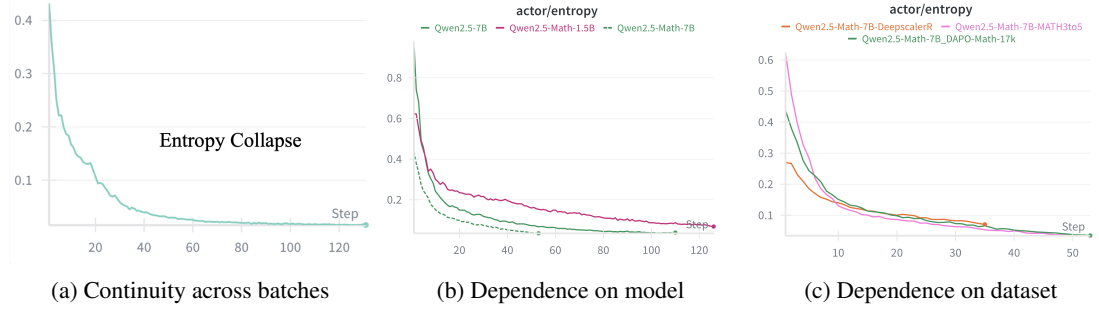


Figure 10: Empirical properties of policy entropy.

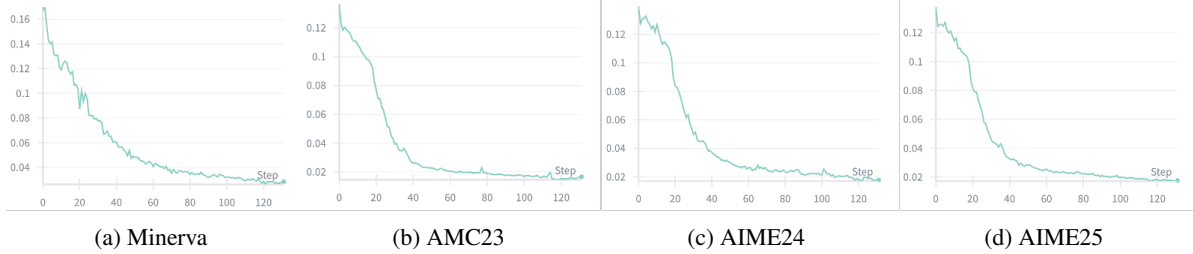


Figure 11: In-domain consistency.

reveals that while all models eventually experience entropy collapse, the initial level and decay speed vary with model size and pretraining. Third, dependence on dataset (panel 3) indicates that training on different math datasets (Math-3to5, DAPO-MATH, DeepScaleR) leads to distinct entropy curves, suggesting that entropy dynamics is also shaped by data distribution and difficulty. Finally, in-domain consistency (panel 4) shows that, within a fixed training run, entropy measured on several test sets in the same domain (Minerva, AMC23, AIME24, AIME25) follows highly similar monotonically decreasing trajectories, implying that a single global entropy trend governs a wide range of tasks. Together, these observations provide an overall picture of how policy entropy behaves in RLVR before any additional intervention is applied.

## C.2 Entropy Change Estimation Comparison

To quantify this gap between entropy change estimator and ground-truth entropy change, we compute the Mean Squared Error (*MSE*), Pearson Correlation Coefficient (*PCC*), and Spearman’s Rank Correlation Coefficient (*SRCC*) between each estimation and the ground-truth token-level entropy change, as shown in Figure 7. Across all three metrics,  $\Omega_{i,t}$  from Theorem 1 delivers orders-of-magnitude lower *MSE* and substantially higher *PCC* and *SRCC* than *Cov*. Furthermore, the *SRCC* between  $\Omega_{i,t}$  and the ground-truth token entropy change exceeds 60% across all models, demon-

strating a strong rank correlation. These results strongly validate the effectiveness of our estimator derived in Theorem 1 and the soundness of Assumption 1. A more comprehensive comparison is provided below.

Model	Method	MSE ↓	PCC ↑	SRCC ↑
Math-1.5B	<i>Cov</i>	5.37	-6e-5	+0.04
	<i>Ours</i>	5e-4	+0.42	+0.65
7B	<i>Cov</i>	0.53	+0.05	+0.08
	<i>Ours</i>	8e-4	+0.39	+0.72
Math-7B	<i>Cov</i>	0.29	+0.03	+0.06
	<i>Ours</i>	4e-4	+0.42	+0.61

Table 7: Comparison of MSE, PCC and SRCC between covariance-based estimator (*Cov*) and *ours*.

We recorded the token entropy changes for the first 10 training steps across different models and datasets. Figure 12 and 13 show the results on dataset DAPO-Math-17k. The curve denotes the estimated vs. ground-truth entropy change (left axis) and histograms show token counts per bin (right axis). It can be observed that our method exhibits a clear positive correlation with ground-truth entropy change, which strongly supports our theoretical framework. By contrast, the estimation

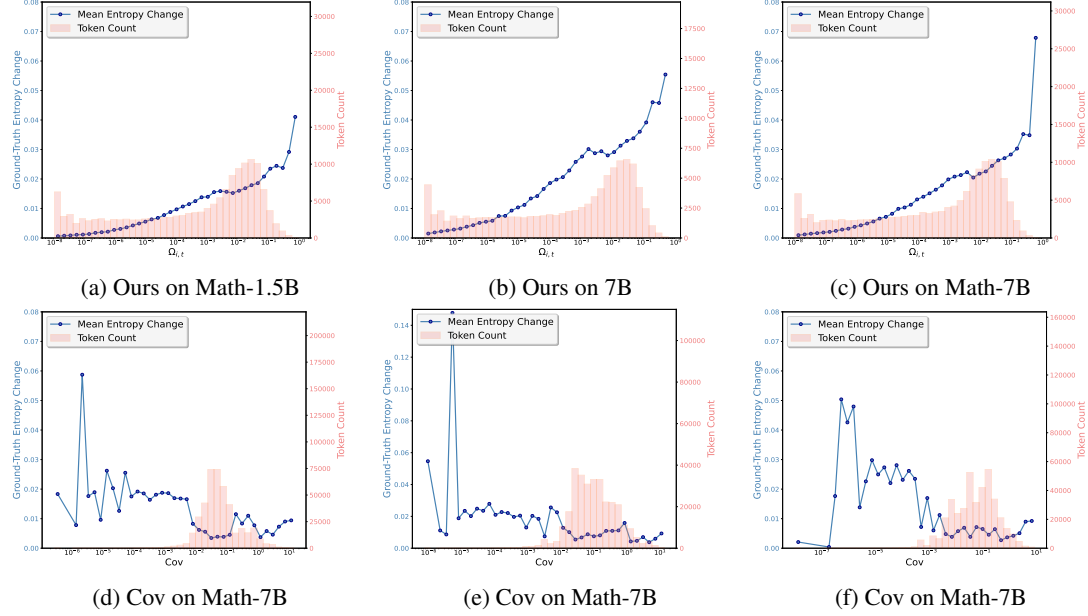


Figure 12: Entropy Change on DAPO-Math-17k.

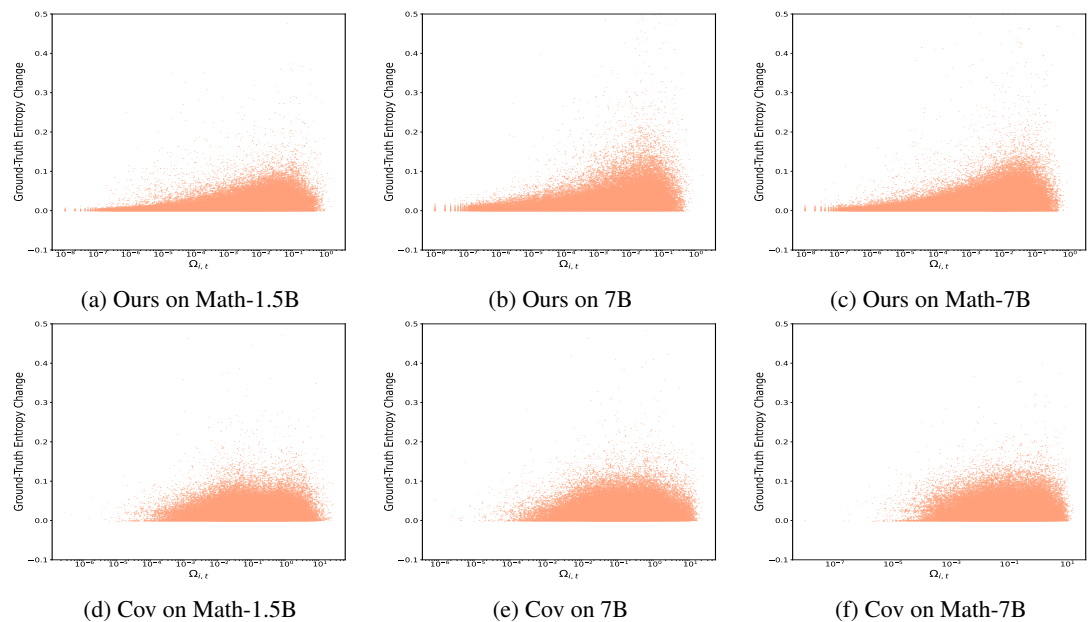


Figure 13: Entropy Change scatters on DAPO-Math-17k.

scheme in (Cui et al., 2025b) exhibits no clear correlation.

### C.3 Influencing Entropy Dynamics by Strengthening or Weakening the Quadrants

We next ask whether these theoretical findings of quadrant-level tendencies can be used to actively steer entropy in practice. Guided by the above quadrant-level tendencies, we design a simple intervention on 10% of tokens in each quadrant to increase entropy: for the entropy-increasing quadrants (II and IV), we double-weight their updates, whereas for the entropy-decreasing quadrants (I and III), we mask their updates, and then track the resulting policy entropy. As shown in Figure 14, all four interventions consistently increase policy entropy compared to the standard GRPO baseline, supporting our analysis. For experiments in Fig-

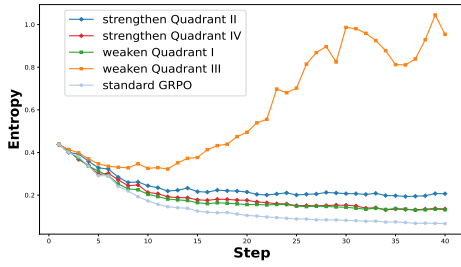


Figure 14: Four schemes to uplift entropy based on advantage-probability effect.

ure 14, we randomly select samples with a generation probability greater than 0.8 and an advantage greater than 0, as well as those with a generation probability less than 0.2 and an advantage less than 0, and randomly mask 10% of such tokens. Similarly, for samples with a generation probability greater than 0.8 and an advantage less than 0, or a generation probability less than 0.2 and an advantage greater than 0, we set the token weight for 10% of such tokens to twice the original token weight.

To further validate the patterns of entropy change with advantage and probability in Figure 2, we strengthen (up-weighting) or weaken (masking) each of the four quadrants at different intensities to induce entropy increases or decreases, respectively. Unlike the setup in Figure 14 where 10% tokens are intervened, we present a more comprehensive validation here.

Figure 15 shows interventions applied to each quadrant with the goal of increasing entropy, using

standard GRPO ( $\varepsilon_{\text{high}}=0.2, \varepsilon_{\text{low}}=0.2$ ) as the baseline; while Figure 16 presents interventions with the goal of decreasing entropy across the four quadrants, using GRPO w/ clip-high ( $\varepsilon_{\text{high}}=0.28, \varepsilon_{\text{low}}=0.2$ ) as the baseline; In each case, the proportion of tokens masked or up-weighted ranges from 5% to 20%. Across all cases, it can be observed that the token-level intervention effects on entropy align with our quantitative analysis framework, and the impact becomes more pronounced as the intervention ratio increases (from 5% to 20%). For example, in Figure 15b, compared to standard GRPO, up-weighting Quadrant II yields a marked increase in policy entropy over standard GRPO (we exclude the 20% up-weight case because it produces excessively high entropy). This indicates that the clip-high mechanism in DAPO (Yu et al., 2025) and unlikeness (He et al., 2025a) can be viewed as a special instance of this intervention. In summary, the overall entropy dynamics arise from the joint contributions of the four quadrants; perturbing any one of them can induce a predictable change in the total entropy from our analysis framework.

### C.4 Entropy Effect of Clipping Operation

In this subsection, we adjust the clipping thresholds to steer entropy change in GRPO, and evaluate RLVR performance under different entropy levels.

The entropy dynamics induced by clip operation is shown in Figure 17. *Clip-high* ( $\varepsilon_{\text{high}}$ ): entropy decreases in the early phase for all settings; larger  $\varepsilon_{\text{high}}$  leads to a clear late-stage entropy rebound and sustained growth, whereas small  $\varepsilon_{\text{high}}$  yields continued decay and low final entropy. *Clip-low* ( $\varepsilon_{\text{low}}$ ): the behavior is more bifurcated—with  $\varepsilon_{\text{low}} = 0.1$ , entropy increases monotonically over training, while  $\varepsilon_{\text{low}} \geq 0.2$  drives entropy rapidly toward (near) zero, exhibiting a much stronger tendency toward entropy collapse.

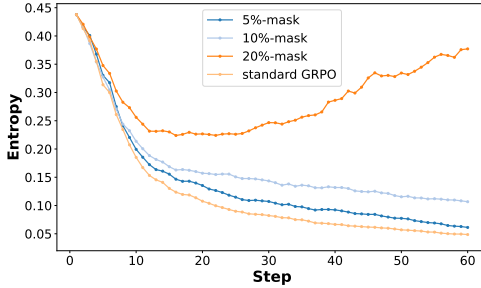
	0.1	0.2	0.5	0.8
$\varepsilon_{\text{high}}$	44.0	44.2	43.7	42.3
$\varepsilon_{\text{low}}$	43.7	44.2	42.5	42.0

Table 8: Average math reasoning performance with different clip operations.

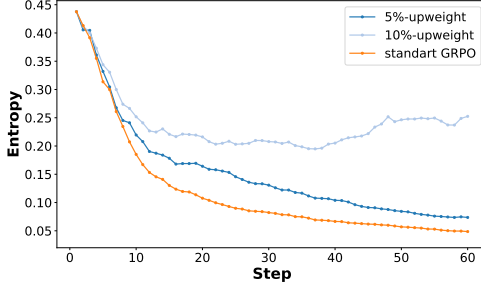
We evaluate these runs individually; the average math reasoning performance under different clipping operations is reported in Table 8. We observe that performance degrades under both entropy col-

Table 9: Dataset statistics.

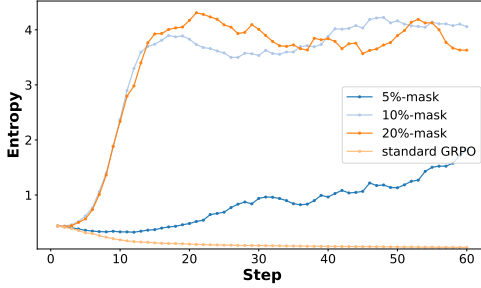
Test Datasets	#Questions	Level
AIME24 (Li et al., 2024)	30	Olympiad
AIME25 (Li et al., 2024)	30	Olympiad
AMC23 (Li et al., 2024)	40	Intermediate
MATH500 (Hendrycks et al., 2021)	500	Advanced
Minerva (Lewkowycz et al., 2022)	272	Graduate
OlympiadBench (He et al., 2024)	675	Olympiad



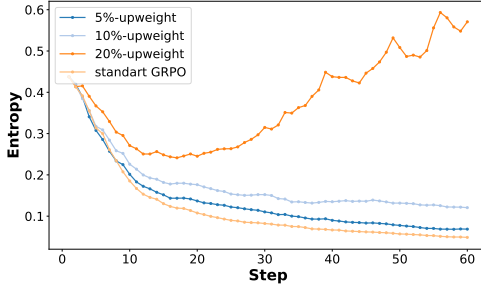
(a) Masking Quadrant I.



(b) Up-weighting Quadrant II.

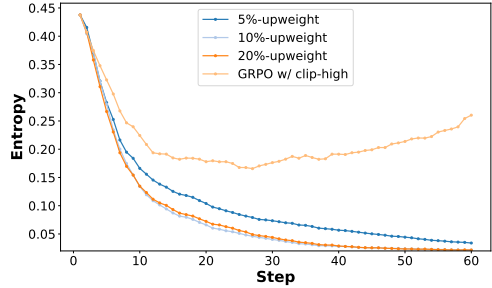


(c) Masking Quadrant III.

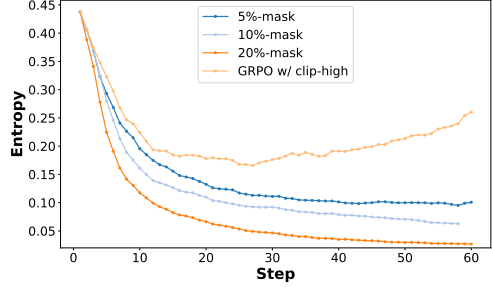


(d) Up-weighting Quadrant IV.

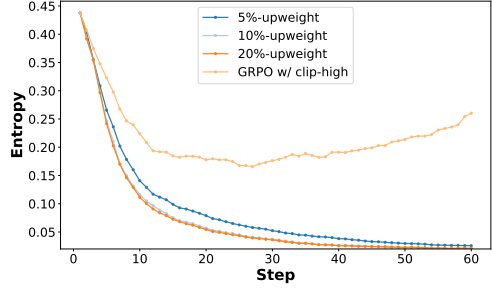
Figure 15: Increasing entropy in four cases.



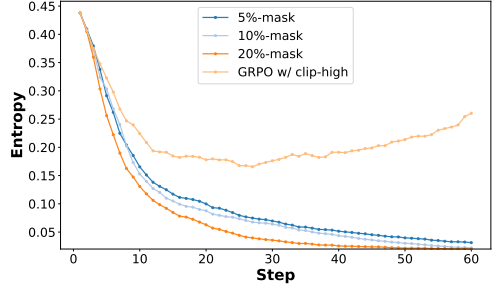
(a) Up-weighting Quadrant I.



(b) Masking Quadrant II.



(c) Up-weighting Quadrant III.



(d) Masking Quadrant IV.

Figure 16: Decreasing entropy in four cases.

lapse and entropy explosion, whereas maintaining entropy within a stable range yields consistently better results. This highlights the importance of stabilizing entropy dynamics, which is aligned with our proposed STEER.

## D Training Settings

### D.1 Detailed Information for dataset

**Math Reasoning** We use DAPO-Math-17k as the training dataset for enhancing model’s math reasoning, which is a competition-style math reasoning dataset introduced in the DAPO work. It contains roughly 17k problem–solution pairs of olympiad-level mathematics (covering algebra, number theory, combinatorics, geometry, etc.), derived from standard public math-reasoning benchmarks and reformatted into supervised trajectories suitable for RLVR training.

Table 9 reports detailed statistics of the test datasets used in our experiments, including the number of questions and difficulty levels. These benchmarks are all widely used to evaluate mathematical reasoning ability.

**Code Tasks** For code generation task, we adopt ArcherCodeR<sup>2</sup> for RLVR training, which contains 6000+ code generation tasks. And we adopt the widely used LiveCodeBench v5 (Jain et al., 2024) for evaluation. As for code edit task, we build a large-scale corpus of practical code-editing examples—over 50000 instances—collected from internal users and representative of their day-to-day software development workflows. We then evaluate the model on both our internal held-out test split (3314 cases) and the Zeta benchmark.

Each example contains two fields: `<prompt>` and `<edit>`. The `<prompt>` field bundles all required inputs, including the surrounding code context, an ordered sequence of prior edits, the target edit span annotated with the cursor position, and any user-provided hints. The `<edit>` field provides the reference (ground-truth) edit.

### D.2 Training Details for our method and baselines

All algorithms are implemented based on the official GRPO codebase within the VeRL framework.

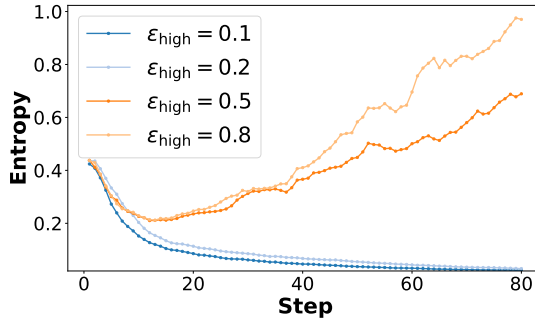
**Training settings** Generation batch size is set to 512, and update batch size is set to 32. The num-

ber of rollouts is set to 8. Both the KL-divergence and entropy loss terms are removed in our experiments. Training is performed with top-p value of 1.0 and temperature is 1.0. We use a learning rate of 1e-6 without warm-up across all experiments. At each rollout step, we generate 8 answers for each of 512 sampled questions with a mini-batch size of 32 for updating policy model. Models are trained for at most 200 rollout steps. Unless otherwise specified, we follow GRPO’s default design choices with token-level loss normalization without dynamic sampling and KL regularization. For Qwen2.5 series models, the maximum input length is 1024 and the maximum output length is 3072. For Qwen2.5-Coder series models in code editing task, the maximum input length is 4096 and the maximum output length is 1024.

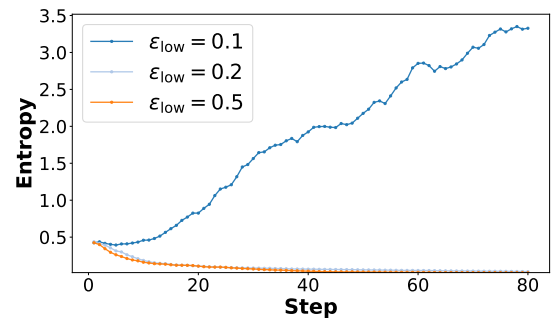
**Evaluation settings** Validation is performed with a top-p value of 0.7 and temperature is 1.0 across all models and test sets. We use Math-Verify and Qwen-Verify for both validation during training and final evaluation. All evaluations are *zero-shot* with no additional prompts. All methods save a checkpoint every 10 steps, and the checkpoint achieving the highest AIME24 accuracy is selected for test. All experiments were conducted on a cluster equipped with NVIDIA H20 GPUs.

**Specific settings for baselines** Table 3 reports the main results, and this subsection details the training setups for all compared baselines. For GRPO (Shao et al., 2024), we follow the official VeRL training recipe and keep all hyperparameters unchanged. For SimpleRL-Zoo (Zeng et al., 2025), we adopt the original training recipe from the official repository, replacing the original math corpus with DAPO-Math-17k as the training data. For Eurus-PRIME (Cui et al., 2025a), we directly use the publicly released checkpoint that is trained on Qwen2.5-Math-7B with process reward. For OPO (Hao et al., 2025), we follow the reference implementation in VeRL without new hyperparameters introduced. GRPO w/ clip-high (Yu et al., 2025) sets the upper clipping threshold to  $\varepsilon_{\text{high}} = 0.28$  while keeping all other settings identical to GRPO. GRPO w/ Entro. Loss (Schulman et al., 2017) augments the GRPO objective with an entropy loss term; we tune its weight over  $\{0.01, 0.001, 0.0001\}$  and report the best result. GRPO w/ Fork Tokens follows the strategy in (Wang et al., 2025c): using only policy gradients of the top 20%, 30%, or 40% highest-entropy to-

<sup>2</sup>Available at <https://huggingface.co/datasets/Fate-Zero/ArcherCodeR-Dataset>.



(a) Effect of  $\varepsilon_{\text{high}}$



(b) Effect of  $\varepsilon_{\text{low}}$

Figure 17: Empirical validation of entropy-change mechanisms via ratio clipping.

kens and report the best-performing configuration. W-REINFORCE (Zhu et al., 2025) is implemented by assigning a reduced weight to positive samples, tuning  $\lambda \in \{0.1, 0.2\}$  and reporting the best result. Entro. Adv. (Cheng et al., 2025) is reproduced following the original paper, fixing  $\kappa = 2$  for all experiments and setting  $\alpha = 0.4$ . Clip-Cov and KL-Cov (Cui et al., 2025b) apply clipping or KL-penalty constraints only to a small subset of generated tokens. Following the original implementation, we set the fraction of constrained tokens to 0.0002.

## E Supplementary Performance Evaluation

This section presents additional performance results that assess the robustness and generality of STEER under varied settings.

### E.1 Performance in Extreme Scenarios

We test entropy intervention methods in uncontrolled training scenarios ( $\varepsilon_{\text{high}} = 5$  and  $\varepsilon_{\text{low}} = 0.99$ ), with test set accuracy shown in Table 10. It can be observed that, even in training scenarios where the clipping operation is almost completely removed, STEER maintains relatively stable performance compared to other entropy intervention methods and achieves the highest accuracy across all test sets.

### E.2 Performance Comparison on Different Models

The performance experiments on Qwen2.5-Math-1.5B and Qwen2.5-14B shown in Table 11 are compared with the top3 competitors in Table 3 (i.e., OPO, Clip Cov, and Entro. Adv.). STEER also consistently achieves the highest average performance on both Qwen2.5-Math-1.5B (38.1) and Qwen2.5-14B (45.1), demonstrating its superior capabilities

in improving model reasoning.

### E.3 Ablation Study

Besides the exponential mapping in Eq. (3), we consider the following linear mapping and binary mapping for ablation:

$$\begin{aligned} \text{linear: } \lambda_{i,t} &= \lambda_{\max} - \frac{\lambda_{\max} - \lambda_{\min}}{\Omega_{\max} - \Omega_{\min}} (\Omega_{i,t} - \Omega_{\min}), \\ \text{binary: } \lambda_{i,t} &= \begin{cases} \lambda_{\min}, & \Omega_{i,t} > Q_{\xi}(\Omega), \\ 1, & \text{otherwise.} \end{cases} \end{aligned}$$

We set  $\lambda_{\min} = 0.7$  throughout and  $\lambda_{\max} = 1.2$  for the linear mapping. For the binary mapping, the quantile threshold  $Q_{\xi}$  is set to  $Q_{0.8}$ —i.e., the top 20% of tokens by  $\Omega_{i,t}$  are assigned weight  $\lambda_{\min}$  and the remaining 80% of tokens keep weight 1. The three mapping schematics are illustrated in Figure 18, and their performance on Qwen2.5-Math-7B is reported in Table 12, each is the average of two runs. It can be seen that the binary mapping degrades performance, whereas the linear mapping does not materially harm performance. This highlights the necessity of continuous token-level reweighting, as truncation cannot precisely control entropy change.

We also assess the sensitivity of the experimental results to hyperparameters  $\lambda_{\min}$  in Eq. (3). An excessively small  $\lambda_{\min}$  may hinder the model’s learning and lead to unstable training, while an excessively large  $\lambda_{\min}$  reduces the model’s ability to control entropy. As shown in Figure 19, our method performs consistently well when  $\lambda_{\min} \in [0.6, 0.8]$ .

Table 10: Performance on test datasets in extreme scenarios.

Method	AIME24	AIME25	AMC23	MATH500	Minerva	Olympiad	Avg.
GRPO	31.6	12.8	66.7	79.0	39.3	40.1	44.9
Entro. Adv.	34.8	13.4	64.3	77.6	37.6	39.9	44.6
Entro. Loss	32.7	14.7	71.3	79.0	36.8	41.4	46.0
Clip-Cov	30.4	14.0	72.3	79.6	37.1	41.7	45.8
STEER	<b>36.1</b>	<b>16.0</b>	<b>76.3</b>	<b>80.5</b>	<b>39.5</b>	<b>42.3</b>	<b>48.5</b>

Table 11: Benchmark results of different methods. We report avg@32 for AIME24, AIME25, and AMC23 and avg@1 for others. All results are presented as percentages.

Method	AIME24	AIME25	AMC23	MATH500	Minerva	Olympiad	Avg.
<b>Qwen2.5-Math-1.5B</b>							
base	4.1	2.1	24.7	29.0	9.2	20.5	14.9
GRPO	16.2	7.6	56.0	74.4	26.1	34.6	35.8
OPO	14.8	9.0	58.2	72.2	26.1	35.9	36.0
Entro. Adv.	15.0	9.1	55.7	70.2	26.8	34.9	35.3
Clip-Cov	14.7	8.4	56.0	72.8	26.4	34.9	35.5
STEER	<b>17.4</b>	<b>9.7</b>	<b>61.6</b>	<b>75.5</b>	<b>28.2</b>	<b>36.6</b>	<b>38.2</b>
<b>Qwen2.5-14B</b>							
base	3.9	2.6	25.8	52.6	15.4	23.0	20.6
GRPO	17.2	13.2	66.3	80.6	38.0	42.2	42.9
OPO	17.8	12.6	68.2	78.6	37.7	42.6	42.9
Entro. Adv.	14.6	9.8	65.6	78.8	36.5	40.9	41.0
Clip-Cov	14.1	13.6	59.8	78.2	38.6	43.2	41.2
STEER	<b>19.3</b>	<b>14.3</b>	<b>70.3</b>	<b>81.4</b>	<b>39.4</b>	<b>46.7</b>	<b>45.2</b>

Table 12: Ablation study on different weight mapping modes.

Mapping	AIME24	AIME25	AMC23	MATH500	Minerva	Olympiad	Avg.
exponential	36.2	16.1	72.1	82.2	41.7	43.0	48.6
linear	36.0	15.7	73.6	81.8	39.4	41.8	48.0
binary	32.5	14.7	71.3	80.9	38.2	41.5	46.5

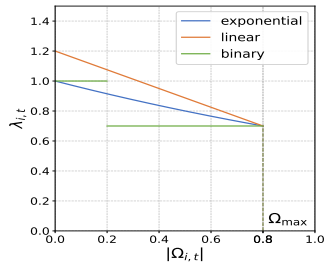


Figure 18: Weight Mapping.

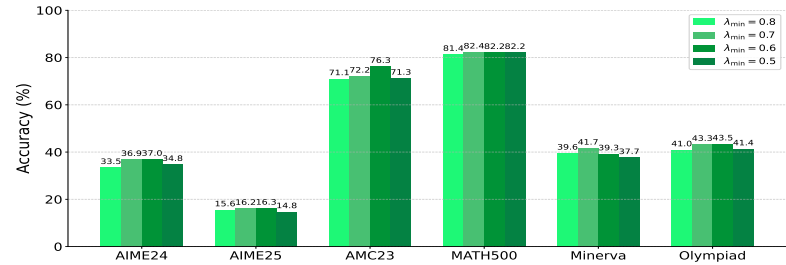


Figure 19: Hyperparameter Sensitivity on  $\lambda_{\min}$ .

## F Theorem Proof Details

During the RLVR training, token logits are shaped by entangled internal parameters, making entropy change difficult to quantify. To capture the essence of distribution shifts during training, we adopt the following weak assumption.

**Assumption 1** (Parameter-independent softmax). *For any context (state)  $s = (q, o_{<t})$ , each token (action)  $a$  in the vocabulary  $\mathcal{V}$  is associated with an independent logit parameter  $z_{s,a}(\theta)$ . At update step  $k$  in training, the next-token distribution of  $\pi_\theta^k$  then follows*

$$\pi_\theta^k(\cdot | s) = \text{softmax}(z^k(s)),$$

where  $z^k(s)$  is the vector of logit parameters for all actions under state  $s$ .

Assumption 1 states that a gradient step on the sampled token does not substantially affect the logits of the other tokens in the vocabulary. Given this assumption, we derive the following theorem on token entropy change.

**Theorem 1** (First-order entropy change estimation). *Let the policy model  $\pi_\theta$  satisfy Assumption 1. For any context (state)  $s = (q, o_{<t})$ , define the token-level entropy change between two update steps as*

$$\Delta\mathcal{H}(s) \triangleq \mathcal{H}(\pi_\theta^{k+1} | s) - \mathcal{H}(\pi_\theta^k | s).$$

Under a single GRPO update in Eq. (1),  $\Delta\mathcal{H}(s)$  admits the decomposition

$$\Delta\mathcal{H}(s) = \Omega(s) + \Phi(s), \quad (7)$$

where the first-order estimation term is

$$\Omega(s) = -\frac{\eta}{L} \mathbb{E}_{a \sim \pi_\theta^k(\cdot | s)} \left[ \frac{\mathbb{I}_{\text{clip}}(s, a) A(s, a)}{\pi_{\text{old}}(a | s)} \pi_\theta^k(a | s) (1 - \pi_\theta^k(a | s)) (\log \pi_\theta^k(a | s) + \mathcal{H}(\pi_\theta^k | s)) \right], \quad (8)$$

and the higher-order remainder term  $\Phi(s)$  satisfies

$$|\Phi(s)| \leq C \eta^2 \left[ \frac{A_{\max} r_{\max}}{L} \right]^2, \quad (9)$$

where  $L$  is the total decoded length in the GRPO update and  $A_{\max}, r_{\max}$  bound the token-level advantage and importance ratio and  $C > 0$  is a constant depending on the policy parameterization.

*Proof.* We prove the theorem in five steps as follows.

**Step 1: First-order Taylor expansion.** Taking the first-order Taylor expansion of  $\Delta\mathcal{H}(s)$  around  $z^k(s)$ , we have

$$\begin{aligned} \Delta\mathcal{H}(s) &= \mathcal{H}(\pi_\theta^{k+1} | s) - \mathcal{H}(\pi_\theta^k | s) \\ &= \underbrace{\left\langle \frac{\partial \mathcal{H}(\pi_\theta^k | s)}{\partial z}, z^{k+1}(s) - z^k(s) \right\rangle}_{\text{first-order term } \Omega(s)} + \underbrace{\mathcal{O}(\|z^{k+1}(s) - z^k(s)\|_2^2)}_{\text{higher-order remainder } \Phi(s)}, \end{aligned} \quad (10)$$

where  $z(s) = (z_{s,a})_{a \in \mathcal{V}}$  is the logit vector for all actions under state  $s$ .

**Step 2: Gradient of entropy w.r.t. logits.** For a fixed state  $s$ , the conditional entropy of the policy  $\pi_\theta^k(\cdot | s)$  is

$$\mathcal{H}(\pi_\theta^k | s) = - \sum_{a \in \mathcal{V}} \pi_\theta^k(a | s) \log \pi_\theta^k(a | s).$$

Under the parameter-independent softmax parameterization, each token  $a \in \mathcal{V}$  has a logit  $z_{s,a}^k$  and

$$\pi_\theta^k(a | s) = \frac{\exp(z_{s,a}^k)}{\sum_{b \in \mathcal{V}} \exp(z_{s,b}^k)}.$$

We differentiate  $\mathcal{H}(\pi_\theta^k | s)$  with respect to a single logit  $z_{s,b}$ . Using the softmax derivative, we have

$$\frac{\partial \pi_\theta^k(a | s)}{\partial z_{s,b}} = \pi_\theta^k(a | s) (\mathbf{1}\{a = b\} - \pi_\theta^k(b | s)).$$

Then, we obtain

$$\begin{aligned} \frac{\partial \mathcal{H}(\pi_\theta^k | s)}{\partial z_{s,b}} &= - \sum_{a \in \mathcal{V}} (\log \pi_\theta^k(a | s) + 1) \frac{\partial \pi_\theta^k(a | s)}{\partial z_{s,b}} \\ &= - \sum_{a \in \mathcal{V}} (\log \pi_\theta^k(a | s) + 1) \pi_\theta^k(a | s) (\mathbf{1}\{a = b\} - \pi_\theta^k(b | s)) \\ &= - (\log \pi_\theta^k(b | s) + 1) \pi_\theta^k(b | s) (1 - \pi_\theta^k(b | s)) + \pi_\theta^k(b | s) \sum_{a \neq b} (\log \pi_\theta^k(a | s) + 1) \pi_\theta^k(a | s) \\ &= - (\log \pi_\theta^k(b | s) + 1) \pi_\theta^k(b | s) (1 - \pi_\theta^k(b | s)) \\ &\quad + \pi_\theta^k(b | s) \left[ \sum_{a \in \mathcal{V}} (\log \pi_\theta^k(a | s) + 1) \pi_\theta^k(a | s) - (\log \pi_\theta^k(b | s) + 1) \pi_\theta^k(b | s) \right] \\ &= - (\log \pi_\theta^k(b | s) + 1) \pi_\theta^k(b | s) + \pi_\theta^k(b | s) \sum_{a \in \mathcal{V}} (\log \pi_\theta^k(a | s) + 1) \pi_\theta^k(a | s), \end{aligned}$$

where  $\mathcal{V}$  denotes the vocabulary. Note that

$$\sum_{a \in \mathcal{V}} \pi_\theta^k(a | s) = 1, \quad \sum_{a \in \mathcal{V}} \log \pi_\theta^k(a | s) \pi_\theta^k(a | s) = -\mathcal{H}(\pi_\theta^k | s).$$

Therefore,

$$\sum_{a \in \mathcal{V}} (\log \pi_\theta^k(a | s) + 1) \pi_\theta^k(a | s) = -\mathcal{H}(\pi_\theta^k | s) + 1.$$

Substituting back, we get

$$\begin{aligned} \frac{\partial \mathcal{H}(\pi_\theta^k | s)}{\partial z_{s,b}} &= - (\log \pi_\theta^k(b | s) + 1) \pi_\theta^k(b | s) + \pi_\theta^k(b | s) (-\mathcal{H}(\pi_\theta^k | s) + 1) \\ &= - \pi_\theta^k(b | s) (\log \pi_\theta^k(b | s) + \mathcal{H}(\pi_\theta^k | s)). \end{aligned}$$

Thus, for any  $a \in \mathcal{V}$ ,

$$\frac{\partial \mathcal{H}(\pi_\theta^k | s)}{\partial z_{s,a}} = - \pi_\theta^k(a | s) (\log \pi_\theta^k(a | s) + \mathcal{H}(\pi_\theta^k | s)). \quad (11)$$

**Step 3: One-step GRPO update in logit space.** The policy gradient of GRPO in Eq. (1) can be written as

$$\nabla_\theta J(\theta) = \mathbb{E}_{\substack{q \sim \mathcal{D}, \\ \{o_i\}_{i=1}^G \sim \pi_{\text{old}}(\cdot | q)}} \left[ \frac{1}{\sum_{i=1}^G |o_i|} \sum_{i=1}^G \sum_{t=1}^{|o_i|} \mathbb{I}_{\text{clip}}(i, t) \frac{\pi_\theta^k(o_{i,t} | q, o_{i,<t})}{\pi_{\text{old}}(o_{i,t} | q, o_{i,<t})} A_{i,t} \nabla_\theta \log \pi_\theta(o_{i,t} | q, o_{i,<t}) \right], \quad (12)$$

where  $\mathbb{I}_{\text{clip}}(i, t)$  is the clipping indicator and  $A_{i,t}$  is the token-level advantage.

For notational convenience, fix a particular token position  $(i, t)$  and write

$$s \triangleq (q, o_{i,<t}), \quad a \triangleq o_{i,t}.$$

We also write  $\mathbb{I}_{\text{clip}}(s, a)$  and  $A(s, a)$  to denote the same quantities as functions of the state–action pair  $(s, a)$ . Under Assumption 1, each logit  $z_{s,a}$  is treated as an independent parameter. Under the softmax parameterization, the derivative of the log-probability with respect to its own logit is

$$\frac{\partial}{\partial z_{s,a}} \log \pi_\theta^k(a | s) = 1 - \pi_\theta^k(a | s),$$

while the derivatives with respect to logits of non-sampled actions  $a' \neq a$  at the same state  $s$  are neglected.

An update of  $z_{s,a}$  in the direction of the GRPO gradient with learning rate  $\eta$  therefore contributes

$$\begin{aligned} z_{s,a}^{k+1} - z_{s,a}^k &= \eta \frac{1}{\sum_{i'=1}^G |o_{i'}|} \mathbb{I}_{\text{clip}}(i, t) \frac{\pi_\theta^k(a | s)}{\pi_{\text{old}}(a | s)} A_{i,t} \frac{\partial}{\partial z_{s,a}} \log \pi_\theta^k(a | s) \\ &= \eta \frac{1}{\sum_{i'=1}^G |o_{i'}|} \mathbb{I}_{\text{clip}}(i, t) \frac{\pi_\theta^k(a | s)}{\pi_{\text{old}}(a | s)} A_{i,t} (1 - \pi_\theta^k(a | s)). \end{aligned} \quad (13)$$

By switching to the  $(s, a)$  notation explicitly, we obtain the simplified update

$$z_{s,a}^{k+1} - z_{s,a}^k = \eta \frac{1}{\sum_{i'=1}^G |o_{i'}|} \mathbb{I}_{\text{clip}}(s, a) \frac{\pi_\theta^k(a | s)}{\pi_{\text{old}}(a | s)} A(s, a) (1 - \pi_\theta^k(a | s)). \quad (14)$$

For non-sampled actions  $a'$  at the same state  $s$ , the corresponding logits  $z_{s,a'}$  remain unchanged in this update.

**Step 4: First-order estimation  $\Omega(s)$ .** Plugging (11) and (14) into the inner product, we have

$$\begin{aligned} \Omega(s) &= \left\langle \frac{\partial \mathcal{H}(\pi_\theta^k | s)}{\partial z}, z^{k+1}(s) - z^k(s) \right\rangle \\ &= \sum_{a \in \mathcal{V}} \frac{\partial \mathcal{H}(\pi_\theta^k | s)}{\partial z_{s,a}} (z_{s,a}^{k+1} - z_{s,a}^k) \\ &= \sum_{a \in \mathcal{V}} \left[ -\pi_\theta^k(a | s) (\log \pi_\theta^k(a | s) + \mathcal{H}(\pi_\theta^k | s)) \right] \left[ \frac{\eta}{L} \frac{\mathbb{I}_{\text{clip}}(s, a) A(s, a)}{\pi_{\text{old}}(a | s)} \pi_\theta^k(a | s) (1 - \pi_\theta^k(a | s)) \right] \\ &= -\frac{\eta}{L} \sum_{a \in \mathcal{V}} \frac{\mathbb{I}_{\text{clip}}(s, a) A(s, a)}{\pi_{\text{old}}(a | s)} [\pi_\theta^k(a | s)]^2 (1 - \pi_\theta^k(a | s)) (\log \pi_\theta^k(a | s) + \mathcal{H}(\pi_\theta^k | s)) \\ &= -\frac{\eta}{L} \mathbb{E}_{a \sim \pi_\theta^k(\cdot | s)} \left[ \frac{\mathbb{I}_{\text{clip}}(s, a) A(s, a)}{\pi_{\text{old}}(a | s)} \pi_\theta^k(a | s) (1 - \pi_\theta^k(a | s)) (\log \pi_\theta^k(a | s) + \mathcal{H}(\pi_\theta^k | s)) \right], \end{aligned}$$

where  $L$  denotes  $\sum_{i'=1}^G |o_{i'}|$  for short. In the last line, we rewrote the sum as an expectation under  $a \sim \pi_\theta^k(\cdot | s)$  by absorbing one factor  $\pi_\theta^k(a | s)$  into the measure. This is exactly Eq. (8).

**Step 5: Remainder term  $\Phi(s)$ .** By multivariate Taylor's theorem, the higher-order remainder can be written as a quadratic form in the logit increment, so there exists a constant  $C > 0$  such that for any state  $s$ ,

$$|\Phi(s)| \leq C \left\| z^{k+1}(s) - z^k(s) \right\|_2^2. \quad (15)$$

For a given state  $s$ , only the sampled action  $a$  has a nonzero logit update, hence

$$\left\| z^{k+1}(s) - z^k(s) \right\|_2^2 = (z_{s,a}^{k+1} - z_{s,a}^k)^2.$$

Denote  $L \triangleq \sum_{i'=1}^G |o_{i'}|$ ,  $r(s, a) \triangleq \frac{\pi_\theta^k(a | s)}{\pi_{\text{old}}(a | s)}$ , and assume the importance ratios and the token-level advantage are uniformly bounded:

$$|r(s, a)| \leq r_{\max}, \quad |A(s, a)| \leq A_{\max} \quad \text{for all } (s, a).$$

Using the GRPO update in Eq. (14), we obtain

$$\begin{aligned}
\left\| z^{k+1}(s) - z^k(s) \right\|_2^2 &= (z_{s,a}^{k+1} - z_{s,a}^k)^2 \\
&= \eta^2 \left[ \frac{\mathbb{I}_{\text{clip}}(s, a) A(s, a)}{L} r(s, a) (1 - \pi_\theta^k(a | s)) \right]^2 \\
&\leq \eta^2 \left[ \frac{\mathbb{I}_{\text{clip}}(s, a) A(s, a)}{L} r(s, a) \right]^2 \\
&\leq \eta^2 \left[ \frac{A(s, a) r(s, a)}{L} \right]^2 \\
&\leq \eta^2 \left[ \frac{A_{\max} r_{\max}}{L} \right]^2,
\end{aligned}$$

Combining this bound with (15) and absorbing all fixed constants into  $C$  yields

$$|\Phi(s)| \leq C \eta^2 \left[ \frac{A_{\max} r_{\max}}{L} \right]^2. \quad (16)$$

Thus the remainder term is of order  $\mathcal{O}(\eta^2)$  and is further suppressed by the per-update normalization factor  $L^{-2}$  in GRPO.

Combining the above steps completes the proof.  $\square$